

Tribological evaluation on Ni₃Al-based alloy and its composites under unlubricated wear condition

Karin Gong^{a,*}, Zhifeng Zhou^b, P.W. Shum^b, Heli Luo^c, Zhiling Tian^c, Changhai Li^a

^a Department of Materials and Manufacturing Technology, Chalmers University of Technology, SE-412 96 Gothenburg, Sweden

^b Department of Manufacturing Engineering and Engineering Management (MEEM), City University of Hong Kong, Kowloon, Hong Kong

^c China Iron and Steel Research Institute Group (CISRI), Beijing 10081, China

ARTICLE INFO

Article history:

Received 15 March 2010

Received in revised form 6 September 2010

Accepted 25 October 2010

Available online 4 November 2010

Keywords:

Friction coefficient

Specific wear rate

Nickel aluminides

Intermetallics

Sliding wear

Wear resistance

ABSTRACT

Friction coefficients and specific wear rates of an existed Ni₃Al-based NAC-alloy with composition of Ni–18.8Al–10.7Fe–0.5Mn–0.5Ti–0.2B (at.%) and its composites reinforced by 6 vol.% Cr₃C₂- and 6 vol.% MnS-particles, respectively were investigated for the initial understanding of sliding wear behaviors of the materials under unlubricated condition. The testing materials were prepared by hot isostatic pressing (HIP) process. Pin-on-Disk (POD) measurements were carried out under room temperature condition. A commercial vermicular graphite cast iron was selected as a reference material. The disks used in this study were made of a grey cast iron as cylinder liner materials of ship engines. The contact pressure of 2.83 MPa and 5.66 MPa were applied in POD tests. The experimental results revealed that the monolithic NAC-alloy has the almost same values of friction coefficient and specific wear rate under the testing condition as compared to a commercial vermicular cast iron. The wear mechanism is probably conducted to its intrinsic deformation mechanism of the Ni₃Al-type of intermetallics. For the composite with 6 vol.% hard Cr₃C₂-particle, wear rate was reduced on both sides of pin and disk up to 50%, comparing to the single phase NAC-alloy at a high load of 5.66 MPa. By an addition of 6 vol.% soft MnS-particle, wear rate of the disk was dramatically decreased and friction coefficient also slightly reduced on the test. But, the wear rate of pin is maintaining as the same level as the monolithic NAC-alloy and the reference vermicular cast iron. The present investigation recognized that it will be potential to develop Ni₃Al-matrix composites reinforced by hard Cr₃C₂- and/or soft MnS-particles for a certain tribological applications, especially other excellent physical, chemical and mechanical properties of the Ni₃Al-based intermetallic materials were considered.

Crown Copyright © 2010 Published by Elsevier B.V. All rights reserved.

1. Introduction

The metallurgy of intermetallic compounds has been developing rapidly, in parallel with new materials needs in the heavy duty diesel industry. For at least the past four decades, research on intermetallic compounds has largely focused upon mechanical properties, involving low temperature ductility and high temperature strength. Of particular interest, the studies of segregation led to a discovery that addition of only ~0.1 wt.% boron raises the tensile elongation of polycrystalline Ni₃Al alloy from zero to over 50% at room temperature [1]. Then followed by macro-alloying process [2–10], the alloys own the comprehensive mechanical properties for industrial applications. They are now serious candidates for structural applications requiring reduced density, excellent fatigue

strength, corrosion/oxidation resistance, and service at temperatures up to perhaps 800 °C.

One of the most attractive engineering properties of Ni₃Al alloys is their increasing yield strength with increasing temperature up to about 650–750 °C. This type of strength behaviour suggested that the Ni₃Al-based intermetallic alloys may have good wear properties in the peak-strength temperature range. Consequently, investigations of their sliding friction and wear were initiated. In fact, a number of laboratory studies have indicated that Ni₃Al-based alloys have significant potential in wear-critical applications, especially in cavitations erosion and in sliding wear at temperature range between 400 °C and 650 °C [11–16]. Authors related those results to the microstructures and mechanical properties of the tested alloys, and summarized that the greater the proportional improvement in yield strength with temperature, the greater the improvement in wear. But so far, the studies on the sliding friction and wear for Ni-aluminides were mostly limited on the laboratory investigation. Further work aimed to industrial applications is needed.

* Corresponding author. Tel.: +46 31 7721261; fax: +46 772 1313.

E-mail address: karin.gong@chalmers.se (K. Gong).

Intermetallic matrix composites (IMC) with hard particles reinforcements are also attractive for wear applications in severe, i.e. chemically aggressive environments. For instance, chromium carbide reinforced Ni₃Al-matrix composite was developed as a new elevated temperature wear resistance material [17]. The work indicated that the microstructures and secondary phase's distribution characteristics in the studied wear-resistant composites are critical factors for its final performance of the material. In the metal carbides, tungsten carbide and chromium carbide are suitable for adding in the matrix as hard particles due to their very high hot hardness and good wetting ability with the matrix. Compared with tungsten carbide, chromium carbide is even more suitable to be used in air, based on its excellent oxidation resistance [18]. Soft particles added composite is also considered in this investigation. It is expected that the function of added particles is probably like the graphite in cast iron, and can effectively decrease wear rate of the materials.

In this work, a Fe-alloyed Ni₃Al compound (NAC-alloy) and its composites with additions of chromium carbide, as hard phase to against friction, and manganese sulfide, as a soft phase to reduce sliding wear, will be studied and evaluated by POD test under non-lubrication condition in air at room temperature, and analyzed by several advanced techniques.

2. Experimental methods

2.1. Testing materials and preparation

A Fe-alloyed Ni₃Al (NAC-alloy) was selected in the work. Composition of the alloy is Ni–18.8Al–10.7Fe–0.5Mn–0.5Ti–0.2B in atomic percentage. The powders of NAC-alloy for hot isostatic pressing (HIP) process were prepared by using Plasma Rotating Electrode Process (PREP) in China Iron and Steel research Institute Group (CISRI). At the starting, the PREP system was evacuated up to 0.1 bar to prevent oxidation of the powders formed. The chamber was then flooded with helium and argon. The electrode rod of the master alloy is accelerated up to the desired speed of rotation, 14,500 ± 500 rpm. An argon/helium plasma arc was ignited. The plasma jet melts tip of the rotating rod. A fusion film was formed on the front end of rod, which disintegrated into small liquid metal droplets as a consequence of the centrifugal force. Due to surface tension the droplets are spherical. On their trajectories towards the chamber wall the droplets solidified rapidly in the inert atmosphere and formed spherical powder particles. The NAC-alloy and its composites were prepared by means of HIP process in CISRI. Sizes of NAC-alloy: Cr₃C₂ and MnS powders are in the range of 45–120 μm. The densities of NAC-alloy, Cr₃C₂ and MnS, used for calculating compositions of the composites in volume percentage are 7.25 g/cm³, 6.68 g/cm³ and 3.99 g/cm³, respectively. The applied HIP process data are 1130–1160 °C as heating temperature under 140 MPa for 3 h. The HIP materials were machined to testing pins. Commercial vermicular graphite cast iron as a piston ring material with a composition in weight percentage of Fe–3.05C–1.20Si–0.85Mn–0.10 ± 0.05P–0.05S–0.65 ± 0.05Mo–0.9 ± 0.05Cu–0.02V–0.03Ti was selected as a reference material in this work. The disks used in this study were made of a grey cast iron. The grey cast iron as liner materials of ship engines has a composition of Fe–3.2C–1.1Si–0.8Mn–0.2P–0.1S–0.02B–1.0Cu–0.22V in weight percentage. The designations of the testing specimens were summarized in Table 1.

2.2. Pin-on-Disk (POD) test

For evaluating friction coefficient and wear resistance of the different testing materials, a conventional Pin-on-Disk tribometer was

Table 1
Designations of the testing materials.

Designation	Composition	Process
Specimen #1	NAC-alloy	HIPing
Specimen #2	NAC-alloy + 6 vol.% Cr ₃ C ₂	HIPing
Specimen #3	NAC-alloy + 6 vol.% MnS	HIPing
Specimen #4	Vermicular cast iron	Casted
Disk	Grey cast iron	Casted

used. The measurements were carried out at room temperature in laboratory air with a relative humidity of about 45%. Grey cast iron disks (diameter 30 mm × 4 mm) as a counterpart were selected. Their surface roughness was determined as less 0.2 μm. The pins of testing materials (diameter 3 mm × 16 mm) were also machining to surface roughness of 0.2 μm. The tests were performed under the applied normalizing loads of 20 N and 40 N, corresponding to the pressure of 2.83 MPa and 5.66 MPa, respectively. For each specified test, three pin-samples of the studied materials were investigated on POD equipment in order to obtain statistical working results. The sliding speed of 8 cm s⁻¹ was selected as a constant value by adjusting the rotation speed (200 rpm) of the disk and the diameter (diameter 8 mm) of wear track. The duration of sliding time lasted 6 h. Wear volumes of the pin-samples were calculated from weight loss during the test by assuming a density of 7.25 g/cm³ of the monolithic alloy (specimen #1), 7.23 g/cm³ and 7.12 g/cm³ of the composites #2 and #3, respectively. The density of the compact cast iron used for calculation is 7.30 g/cm³. Wear volumes of the disks were measured accurately by using a computerized three-axis profilometer (Taylor Hobson). Wear tracks of the disks were mapped also. The measured results on wearing in this work are reported in terms of Archard's specific wear rate (mm³/N·m), calculated by the following formula:

$$\text{specific wear rate} = \frac{V}{F \cdot S} \quad (1)$$

where V is the volume worn away in mm³, F is the normal load in N, and S is the sliding distance in meter.

2.3. High temperature hardness measurement

High temperature heating device instrument was used to measure AKASHI-Vickers hardness of NAC-alloy and reference materials cast iron under room temperature and various high temperatures in vacuum chamber. The specimens were made of dimension in a shape of Ø 10 mm × 5 mm; the measuring surface should be mirror-finished and cleaned with acetone. The applied load is 10 kg, and room temperature, 200 °C, 400 °C and 600 °C were selected in final steady state condition.

2.4. Analytical works

The HIPed testing samples were analyzed by a D8 advance X-ray diffraction spectrometer to identify phase constitution of the materials. The Cr-Kα X-ray radiation (wavelength 2.28970 Å) used to get the diffraction pattern of the analyzed specimens. A scanning electron microscope was utilized to evaluate quality of the HIPed materials and other testing samples. The backscattering electron image technique of SEM based on the composition contrast principle and EDS were used for investigating microstructures and quantitative analysis. The results from the analytical works will be coupled to the experimental data of the tribological tests for understanding and evaluation of the studied materials on their wear behaviors.

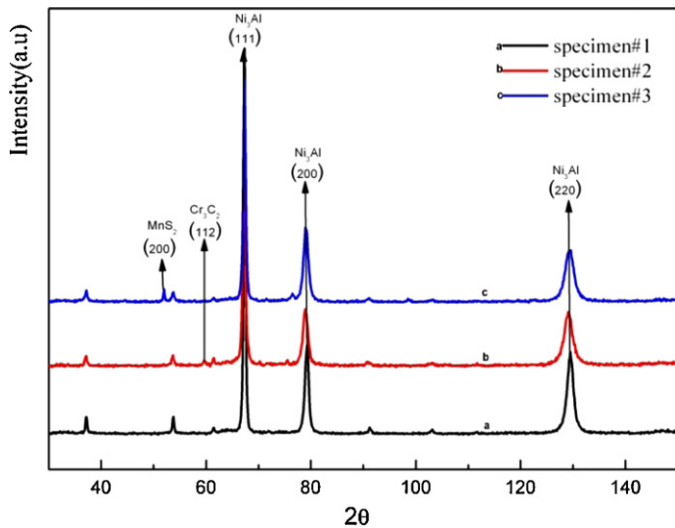


Fig. 1. XRD-spectra analyzed of HIPed NAC-alloy and its composites.

3. Results

3.1.1. Analysis on the testing materials before POD test

For determining the phase constitution of the prepared specimens, X-ray diffraction was performed on the HIPed monolithic NAC-alloy and its composites. The results were collected in Fig. 1. The diffraction spectrum of the specimen #1 revealed that the monolithic NAC-alloy was a single phase material having a Ni₃Al-type (L1₂) crystal structure with a main peak at $2\theta = 67.1^\circ$, derivative of the face-centered cubic (fcc) crystal. The diffraction spectrum of the specimen #2 indicated that two phases as Cr₃C₂-type ($2\theta = 59.52^\circ$ of main peak) and Ni₃Al-type crystal struc-

tures existed in the specimen. In the specimen #3, MnS-phase ($2\theta = 51.99^\circ$ of main peak) and Ni₃Al-phase are existed.

The microstructure observation indicated that the HIPed testing materials reached almost full density and well bonding between the matrix and added phases. Also, the reinforcements are homogeneously distributed on the matrix. Fig. 2a–d is the backscattering electron images (BEI) from the polished non-etched specimens #1, #2, #3 and #4, respectively. Fig. 2a shows a single phase microstructure of specimen #1, as identified by the X-ray diffraction. Fig. 2b recognized two major phases on microstructure, the alloyed Ni₃Al-matrix (bright) and Cr₃C₂ reinforcement particles (black), and also a diffusion area (grey) located between those two major phases, which was formed during the thermal heating by HIP process. The phases were confirmed by point-analysis of EDS also, and published in our earlier work [19]. Fig. 2c shows two phases of Ni₃Al-matrix and added MnS particles (black) in specimen #3, which were also conformed by relatively EDS point analysis. A vermicular morphology of graphite (black) on a non-etched cast iron specimen #4 was shown in Fig. 2d. The graphite functions as a solid lubricant on a fine pearlite matrix of the cast iron. In principle, the added MnS particles in Fig. 2c were expected to work in a similar way as the graphite in Fig. 2d, but on the different matrices, the Ni₃Al-intermetallics phase as matrix in specimen #3 and the fine pearlite matrix of the vermicular cast iron in specimen #4.

3.1.2. Surface observation on the tested intermetallic materials after POD test

Fig. 3a–c is the secondary electron images of specimens #1–#3 after POD test, respectively. The different surface morphology was observed. The worn surface of the monolithic NAC-alloy #1 is rough, see Fig. 3a. With reference to its backscattering electron image (Fig. 4a), the average atomic number of materials on surface asperities is lower, compared with the matrix. EDS analysis revealed that the asperities have various chemical compositions,

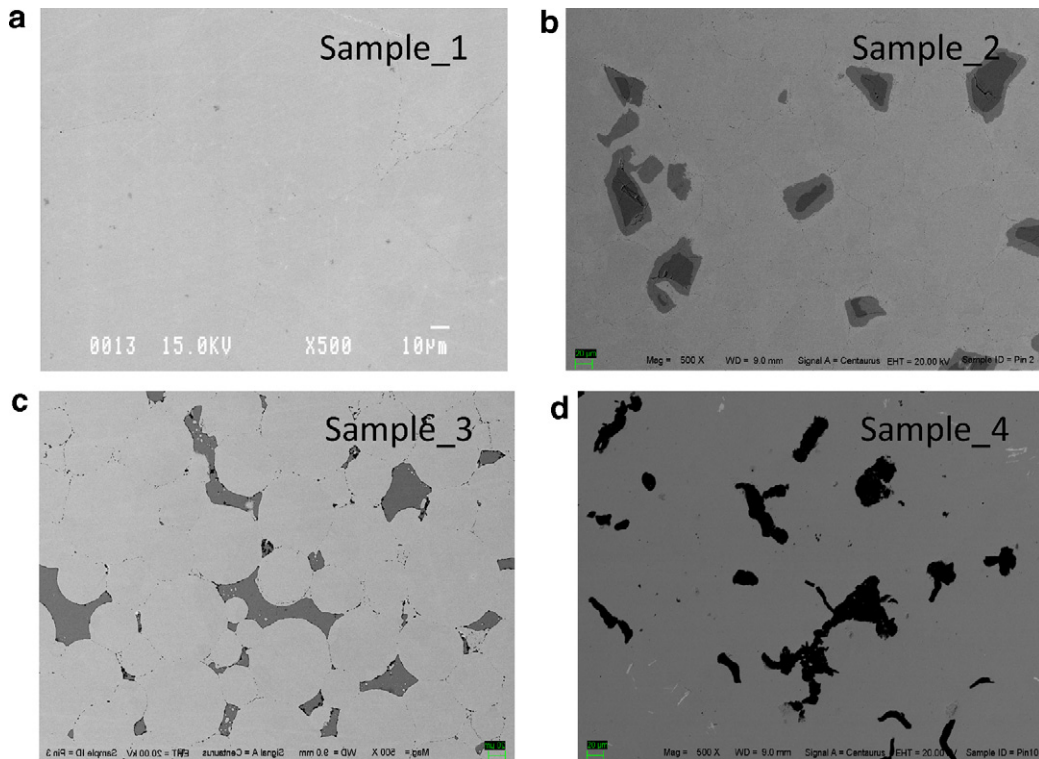


Fig. 2. Backscattering electron images of the testing specimens #1–#4 before POD test.

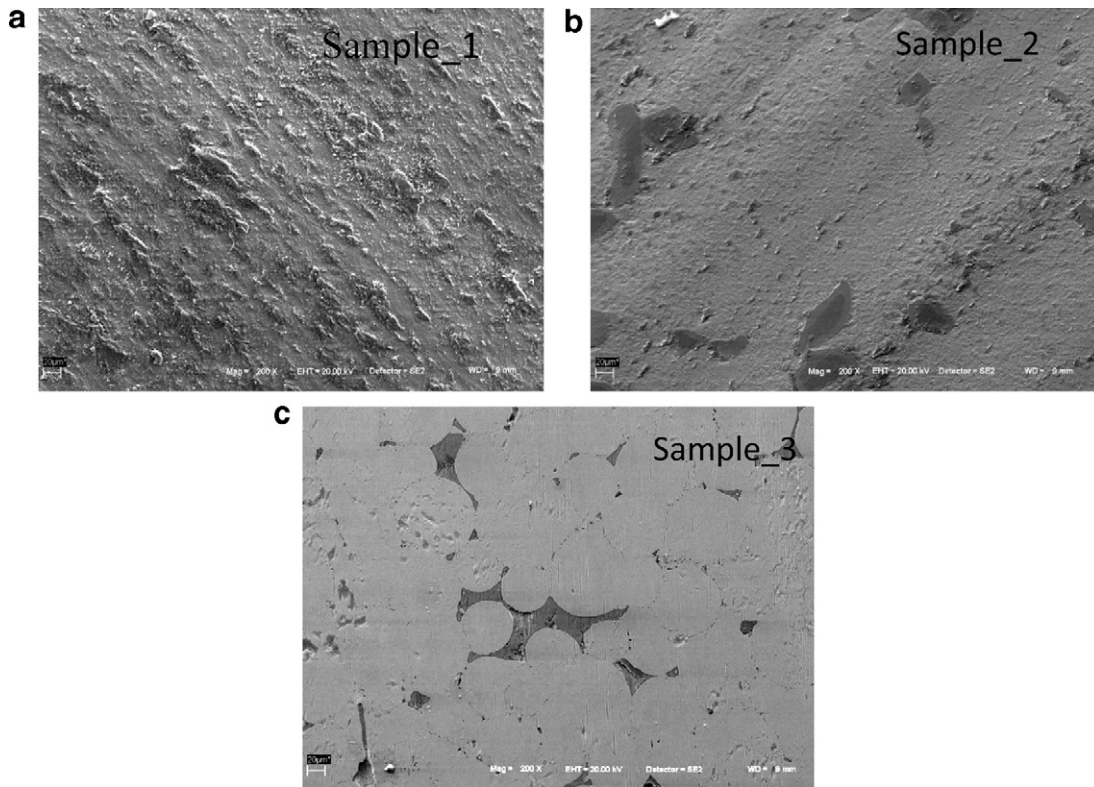


Fig. 3. Secondary electron images of the specimens #1–#3 after POD test.

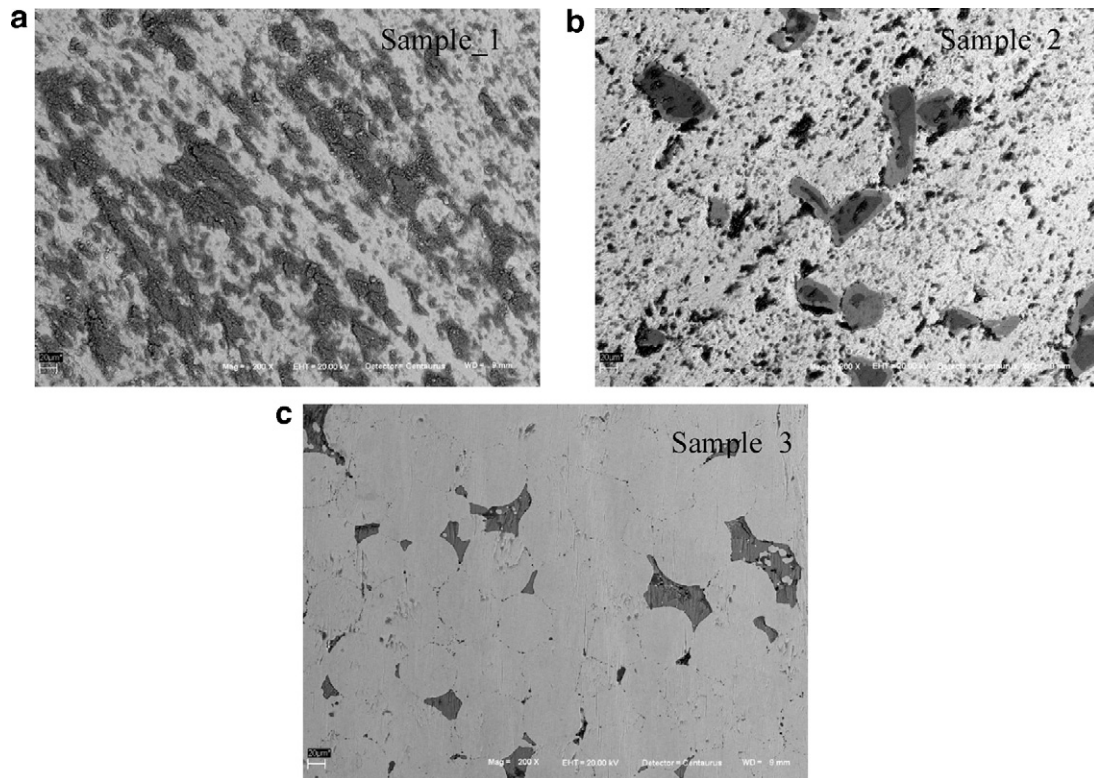


Fig. 4. Backscattering electron images of the specimens #1–#3 after POD test.

Table 2
Friction coefficients and specific wear rates from POD test.

Pin material	Friction coefficient		Specific wear rate (mm ³ /N·m) in 40 N load	
	20 N	40 N	Pin ($\times 10^{-5}$)	Disk ($\times 10^{-6}$)
Specimen #1	0.55 \pm 0.02	–	1.38	11.01
Specimen #2	0.68 \pm 0.02	–	0.76	5.18
Specimen #3	0.45 \pm 0.02	0.32 \pm 0.02	1.54	2.07
Specimen #4	0.58 \pm 0.02	–	1.50	3.03

differ from both of the pin and disk. It means that a serious materials transfer process by local deformation, microcutting and mixing were initiated due to wearing. On the worn surface of the carbide particles added composite #2, much less materials transfer was observed, Fig. 4b. Instead, the carbide particles were kept on the worn surface, Fig. 3b. The worn surface of MnS-particles added composite #3 is smooth, and rare to identify wear tracks, Fig. 3c. The backscattering electron image (Fig. 4c) seems to show that the formed hard debits were not stuck on the worn surface during wearing process, due to a lubrication function of MnS-particles.

3.2. Tribological tests

3.2.1. Friction coefficient

The variations of steady-state friction coefficients of the pin materials (#1–#4), as a function of sliding time, were investigated under two loads of 20 N and 40 N, respectively. The experimental data were collected in Fig. 5 and indicated that the tested materials #1 and #2 have a measurable friction coefficient under 20 N, but the recorded data of the friction coefficient under 40 N was increased dramatically in a short sliding time at the beginning of the test, and

then interrupted measurement quickly, see Fig. 5a and b. Similar trends were also found on the reference material #4 under 40 N in Fig. 5d. There is only one exception from specimen #3. In contrast to other tested materials, the specimen #3 with MnS-addition exhibited a relatively high friction coefficient 0.45 \pm 0.02 under 20 N, and then dropped down to 0.32 \pm 0.02 at 40 N. Thereafter, a load of 20 N was applied to determine the relevant values of friction coefficient from the different tested specimens in this work. And, the statistic data were given in Table 2. Comparing to the commercial wear-resistant vermicular cast iron pin #4, the monolithic NAC-alloy pin #1 has almost the same friction coefficient. The added MnS-particles reduced friction coefficient of the composite obviously, over 15%. But, the hard Cr₃C₂-particles increased the friction coefficient of the composite, more than 20%. It is clearly that the functions of MnS- and Cr₃C₂-particles in the composites are various in sliding wear proceeding. And, it seems that MnS-particles have a role as a kind of solid lubricant in the tested material. It was also interest to notice that friction coefficient of composite #3 with MnS-particles was reduced by increasing load from 20 N to 40 N. Clearly, the phenomenon was not induced by the intrinsic properties of monolithic NAC-alloy, as the performance of speci-

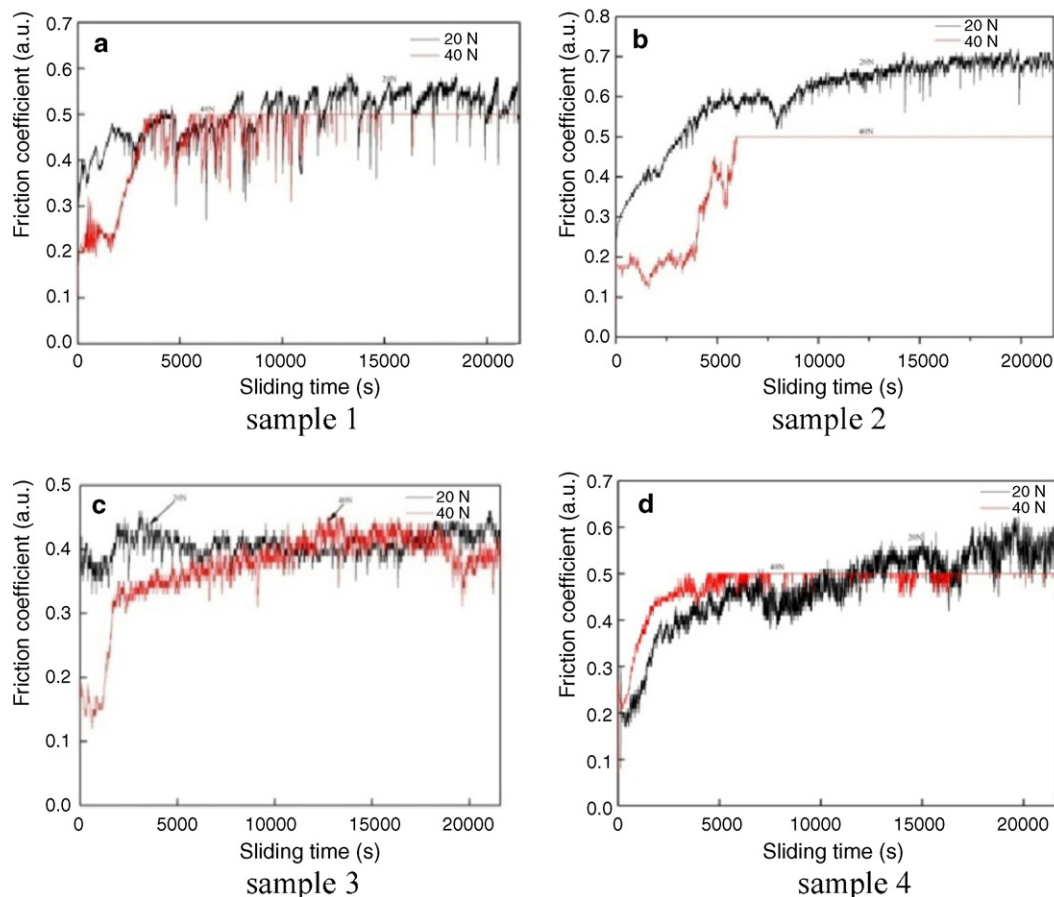


Fig. 5. Steady state friction coefficients vs. sliding time in 6h in various loads of 20 N and 40 N.

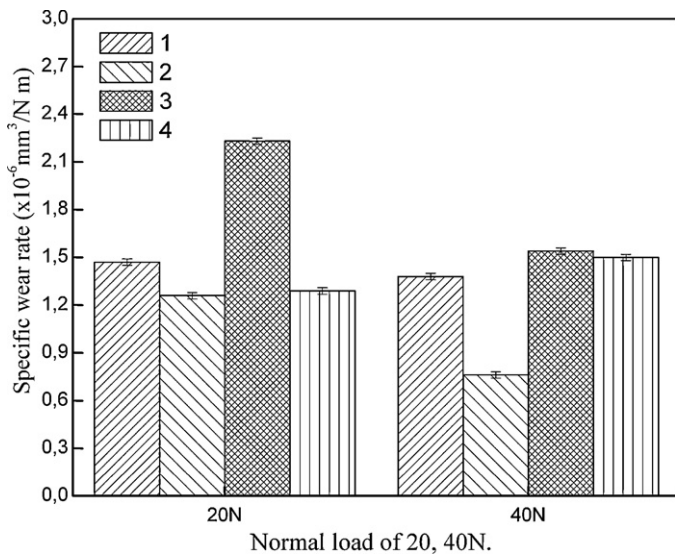


Fig. 6. Specific wear rate vs. testing specimens under two normalized loads of 20 N and 40 N.

men #1 was considered comparatively. Perhaps, it revealed that MnS-particles were working as an effective solid lubricant for the Ni₃Al-matrix composites.

3.2.2. Wear rate

3.2.2.1. Specific wear rate of pin materials. Wear rate of the testing materials were carried out under the loads of 20 N and 40 N in non-lubricated condition, respectively. The calculated values of specific wear rates are given in Fig. 6. Of the monolithic NAC-alloy #1, a wear rate of $1.47 \times 10^{-5} \text{ mm}^3 \text{ N}^{-1} \text{ m}^{-1}$ is for 20 N and $1.38 \times 10^{-5} \text{ mm}^3 \text{ N}^{-1} \text{ m}^{-1}$ for 40 N. The same tendency of decreasing wear rate with increasing applied load has been also observed on specimens #2 and #3, respectively. In the group, the wear rate of specimen #2 was mostly decreased from $1.26 \times 10^{-5} \text{ mm}^3 \text{ N}^{-1} \text{ m}^{-1}$ of 20 N to $7.62 \times 10^{-6} \text{ mm}^3 \text{ N}^{-1} \text{ m}^{-1}$ under a higher load of 40 N. In contrast to the tested intermetallic Ni₃Al-based materials, the metallic vermicular cast iron #4 owned a slightly increased wear rate $1.5 \times 10^{-5} \text{ mm}^3 \text{ N}^{-1} \text{ m}^{-1}$ of 40 N load, compared to $1.29 \times 10^{-5} \text{ mm}^3 \text{ N}^{-1} \text{ m}^{-1}$ of 20 N. Normally, wear rate of the metallic materials will have increased value under a higher load, like

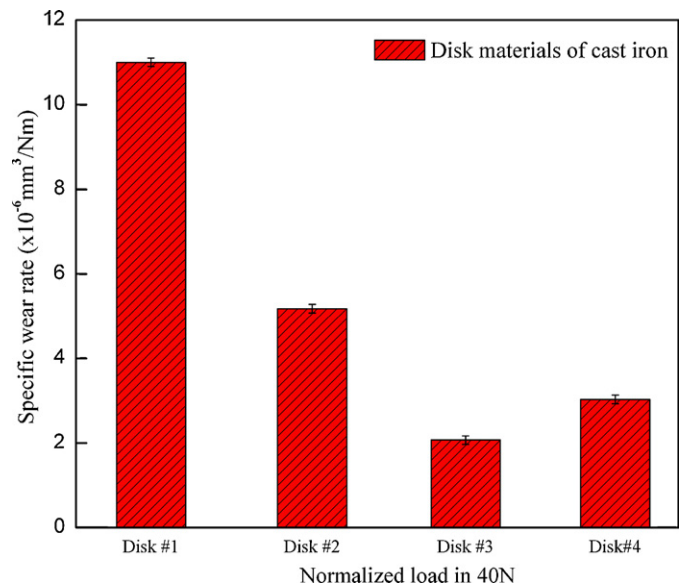


Fig. 8. Specific wear rates of the disks under normalized load of 40 N.

the vermicular cast iron #4. The anomalous behavior of the Ni₃Al-based materials on wear rate under different applied loads probably means that the wear mechanisms of intermetallic and metallic materials are different, which may relate to their varied deformation procedure of sliding wear.

3.2.2.2. Specific wear rate of disk materials. 3D images of the worn disks under loads of 20 N and 40 N were performed. And, the wear loss area of the disks was measured in 3D images by a profilometer. Fig. 7 shows 3D images of the disks from 40 N tests, and revealed that the disk #2 worn by pin #2 has severe and deeper wear tracks on the surface, but less worn volume, compared to the disk #1. It seems to reveal that the added hard particles of Cr₃C₂ in pin #2 formed asperities on the worn pin surface, which have made the deep tracks on the counterpart disk surface, but reduced wearing. The worn surface of the disk #3 is smooth by wearing against MnS-particles added composite. The result was most probably due to an effect of MnS-particles as a soft solid lubricant.

The calculated specific wear rates of the disks to the corresponding pins were given in Fig. 8. But unfortunately, there were not

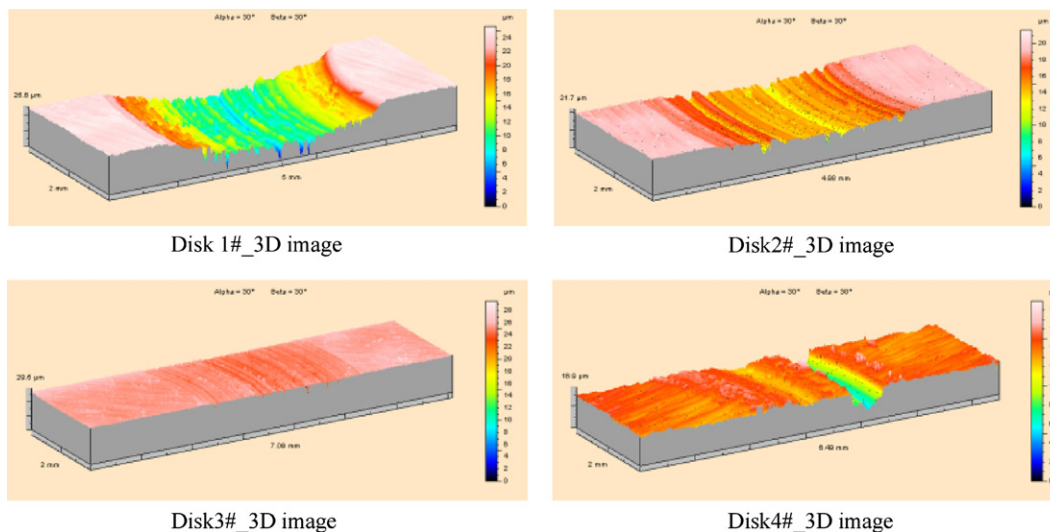


Fig. 7. 3D images of the counterpart disks under load of 40 N.

Table 3
Calculated surface temperature rise under different normal loads.

Normal load	20 N	40 N
a (μm)	66	94
μ (initial)	0.55	0.55
ΔT ($^{\circ}\text{C}$)	159	318

obtained any measured values under 20 N. They are probably due to a short sliding time under this load. Comparing to specific wear rate ($3.03 \times 10^{-6} \text{ mm}^3/\text{N}\cdot\text{m}$) of the disk against the vermicular cast iron #4 under 40 N, only the MnS-particles added composite #3 made a less wear rate ($2.07 \times 10^{-6} \text{ mm}^3/\text{N}\cdot\text{m}$) of the related disk. The monolithic NAC-alloy #1 and its composite #2 reinforced by Cr_3C_2 -particles worn their counterparts faster than the vermicular cast iron #4 made. The specific wear rates of the corresponding disks are $11.01 \times 10^{-6} \text{ mm}^3/\text{N}\cdot\text{m}$ and $5.18 \times 10^{-6} \text{ mm}^3/\text{N}\cdot\text{m}$, respectively. Anyways, the Cr_3C_2 -particle added composite #2 was friendlier working with the counterpart disk, comparing with the monolithic NAC-alloy specimen #1. The measured specific wear rates on the tested pins and disks under the load of 40 N were also listed in Table 2.

3.3. Calculation of flash temperature at contact area

The frictional heating is a general phenomenon in sliding wear tests [20]. To investigate the effect of friction heating on the structure and wear behaviors of pin and disk under different wear conditions (e.g. load), the flash temperature at the contact area is estimated in the present study by the following formula [21].

$$\Delta T = \frac{\mu P v}{4(K_1 + K_2)a} \quad (2)$$

$$a = \left(\frac{P}{\pi H_d} \right)^{1/2} \quad (3)$$

where ΔT is the induced temperature rise, μ the friction coefficient, P the applied normal load, v the sliding speed, K_1 and K_2 the thermal conductivities of the pin and the disk, respectively, a the contact radius of the real contact area, and H_d is the measured hardness of the disk.

It can be seen, the determination of the thermal conductivities of the two bodies in contact is important for the calculation of temperature rise. According to the literatures [22,23], the thermal conductivities of the pin (K_1) and cast iron disk (K_2) are approximately $28.85 \text{ W m}^{-1} \text{ K}^{-1}$ and $55 \text{ W m}^{-1} \text{ K}^{-1}$, respectively. Applying the above data, the flash temperature rise at the contact area can be calculated using Eqs. (2) and (3) under different loads, and the results are listed in Table 3. Therefore, the calculation indicated that at the beginning of sliding, the flash temperature at the local asperity contact is estimated to be lower than 400°C under the tribotesting condition in the present study. It is expected that the temperature at the contact asperities may be raised further by the heat accumulation through repeated friction in the subsequent sliding.

For this reason, the measurement of high temperature hardness variation of surfaces pin and disk were significantly important. Therefore, hardness of the pin NAC-alloy and disk material under the room temperatures, 200°C , 400°C and 600°C , was carried out, and shown in Fig. 9. At room temperature, the initial values of disk hardness $H_{V10}(d) = 237$ and pin hardness $H_{V10}(p) = 224$ were obtained, and the ratio $H_{V10}(d)/H_{V10}(p) > 1$. The hardness of pin #1 was increased by raised temperature. Meanwhile, hardness of the disk cast iron was decreased. Thereafter, the ratio of $H_{V10}(d)/H_{V10}(p) < 1$ was changed.

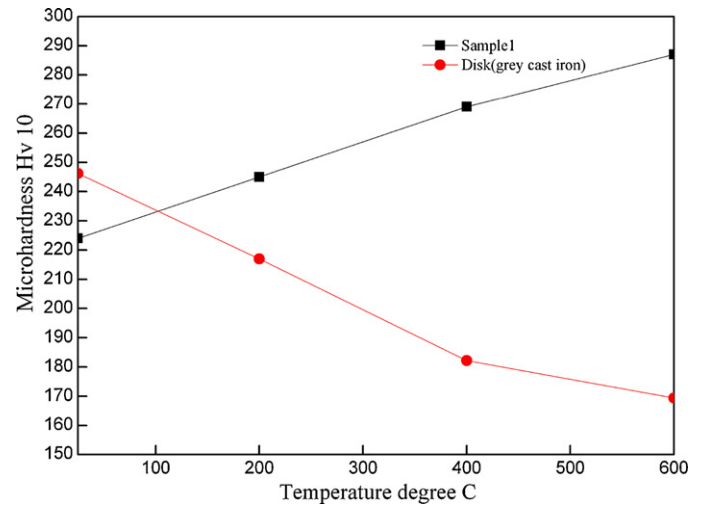


Fig. 9. High temperature hardness variations of NAC-alloy and disk cast iron.

4. Discussion

It is well known that the vermicular graphite cast iron has an optimized phase constitution and microstructure for its acceptable wear resistance by ship engine industries. Pearlite matrix of the vermicular graphite cast iron consists of very hard cementite and bonded by ferrite, formed a fine lamellar microstructure. The hard cementite in the cast iron will have a function to against wearing mostly, assisted by graphite as a solid lubricant. But, the single phase NAC-alloy selected in this work even has a little less specific wear rate. Therefore, it will be reasonable to consider that the wear mechanisms of the vermicular graphite cast iron and the single phase NAC-alloy are various, and to acknowledge that a wear-resistant hard layer on the NAC-alloy was formed during the friction procedure.

From the works [24–26], it has suggested that the sliding wear of metals commonly includes the following sequence of events: large plastic strains resulting from asperity contacts, generation of a heterogeneous substructure consistent with large strains, shear instability leading to transfer of material from one sliding component to the other, mechanical mixing which produces an ultra-fine grain size material on the surface, and removal of this mechanically mixed material as wear debris particles. Therefore, mechanical properties are very important related to the wear behaviour of materials. Especially, the strength of material and its work-hardening behaviour to plastic flow will control the extent of plasticity in the contact region.

Many research works [27–30] were concentrated on the mechanisms of anomalous hardening of the Ni_3Al -based intermetallics. The phenomena were successfully explained on an immobilized action by cross-slip and thermal activated process of superdislocations in L_{12} crystalline structures of the Ni_3Al -type alloys. It has been suggested that the high hardening rate in the ordered crystals may be due to the generation of antiphase domain boundary (APB) tubes formed by cross-slip pinning. The APB and/or stacking fault energy of different lattice plans in ordered structures change with temperature. When the difference is lower following raised temperature, the cross-slipping of the screw dislocations occurs more easily and finally results in high strain hardenability. In fact, the selected NAC-alloy has constant yield strength of not less than 600 MPa up to 600°C , and over 5% room temperature tensile elongation. The alloy has also a higher work-hardening [31], which means that a deformation induced hard layer at the worn surface can be formed quickly, and the hardness of the layer even further raised by an increased surface temperature from friction.

The importance of the relative hardness of the pin and disk was emphasized by works [32,33]. When the fraction ratio of H_d/H_p was less than one, properly severe wear was occurred soon after the start of testing, friction was high and the friction trace contained large fluctuations. With the initial value of H_d/H_p greater than one, two cases will be occurred. In one case, sliding was smooth with low friction throughout the test. The second case began in the same way, but there was then a transition, with subsequent behavior like that observed when the initial value of H_d/H_p is less than one. In the present test on pin #1 with the cast iron disk, the ratio H_d/H_p at room temperature is greater than 1, but value of the ratio was decreases by the increasing surface temperature, resulting $H_d/H_p < 1$. A high work-hardenability of the NAC-alloy will further decrease the ratio. Clearly, the observed severe wear on the disk was related to the low hardness ratio on the worn surface, $H_d/H_p < 1$. The relatively higher specific wear rate of pin #1 probably also conducted to the serious wearing of the disk due to frictionally induced hard debits. Therefore, it is believed that the NAC-alloy as a single phase material will not be as a potential candidate for certain applications in practice. But, it can probably be suitable as a matrix material to develop wear-resistant composites.

It is known that the hard-phase reinforcements can improve wear resistance of metal-matrix composites effectively. Our earlier work [19] also revealed that the added Cr_3C_2 -particles improved wear properties of Ni_3Al -based alloy. But for the composites containing hard particles, it has been also noticed that sliding against a metal counterface resulted in generation of metal filings due to microcutting. Then, these filings were compacted during sliding to form a transfer layer and caused serious wearing results. Lubrication could help to avoid this problem. Unfortunately, this is not the case for a marginal lubrication condition of some engine components. In the present work, a further investigation of Cr_3C_2 -effect on tribological behaviour of the NAC-alloy composite was performed. Also, the influence of the added hard particles on the counterpart was also investigated in the study.

The diffusion zone formed at the interface between the Cr_3C_2 -particle and the NAC-alloy matrix during the thermal and mechanical process of HIP, which made a strong bonding of the particles and matrix, and benefits wear resistance of the material. 6 vol.% Cr_3C_2 -particles addition has lowered the specific wear rate to $0.76 \times 10^{-5} \text{ mm}^3/\text{N}\cdot\text{m}$. Comparing to a specific wear rate $1.38 \times 10^{-5} \text{ mm}^3/\text{N}\cdot\text{m}$ of the single phase NAC-alloy, the reduction of wear rate is effective due to the added hard particles working as a wear-resistant phase. At the same time, the Cr_3C_2 -particles addition also decreased specific wear rate of its counterpart disk to $5.18 \times 10^{-6} \text{ mm}^3/\text{N}\cdot\text{m}$, instead of $11.01 \times 10^{-6} \text{ mm}^3/\text{N}\cdot\text{m}$ of the disk worn by monolithic NAC-alloy without addition of Cr_3C_2 -particles. The added hard particles reduced wearing on both sides of pin and disk, around 50%. On the other hand, Cr_3C_2 -particles addition increased friction coefficient of NAC-alloy to 0.68 ± 0.02 . In the case, it would be logical to consider that the hard Cr_3C_2 -asperities increased the friction resistance, but kept sliding surfaces apart after some parts of the NAC-alloy matrix being worn-off during the wearing process, and avoided direct contact between NAC-alloy matrix and the disk, then reducing the specific wear rates on both sides.

6 vol.% MnS-particle additions even reduced friction coefficient of the NAC-alloy to a value of 0.45 ± 0.02 . On the specific wear rate, the MnS-particles added composite has a value of 1.54×10^{-5} under 40 N, which is slightly higher than 1.38×10^{-6} of the single phase NAC-alloy. But, wear rate of the related counterpart disk is $2.07 \times 10^{-6} \text{ mm}^3/\text{N}\cdot\text{m}$ which is much less than 11.01×10^{-6} of the disk against the single phase NAC-alloy. Also, the worn surface of the related disk is rather smooth with less wear track tails, comparing to the disks worn by other three different pins. Therefore, it will be reasonable to consider that the MnS-particles in the NAC-alloy

composite functioned as a type of solid lubricant. In fact, it was identified in this work by the X-ray diffraction spectrum that MnS-phase has a hexagonal crystalline structure similar to the commonly used solid lubricants of graphite and MoS_2 .

In general, the experimental data recognized that the 6 vol.% MnS-particles added NAC-alloy composite has the same specific wear rate as a commercial vermicular graphite cast iron, but a lower friction coefficient against a liner grey cast iron material, which made itself sliding with the selected counterpart friendlier.

5. Conclusions

From the investigation, several points can be concluded as:

1. The selected single phase NAC-alloy in this work has the almost same friction coefficient and specific wear rate under the testing condition, comparing to a commercial vermicular cast iron used in ship engines. The wear mechanism is most probably conducted to its intrinsic deformation mechanism of the Ni_3Al -type of intermetallics.
2. Unfortunately, the single phase NAC-alloy was not working with its counterpart grey cast iron disk friendly. Therefore, the monolithic NAC-alloy material shall not be applied to a certain wearing condition. But, it can probably be suitable as a matrix material to develop wear-resistant composites.
3. 6 vol.% MnS-particle addition, as an effective solid lubricant, dramatically improved specific wear rate of the grey cast iron disk, and also friction coefficient of the friction-pair. But, its specific wear rate is remained as the same as the monolithic NAC-alloy and the reference vermicular cast iron.
4. Definitely, 6 vol.% added Cr_3C_2 hard particles reduced wearing on both sides of pin and disk, around 50%. It was considered that the hard Cr_3C_2 -asperities kept the sliding surfaces apart, when the matrix part was worn off during the wearing process, then reducing the specific wear rates of both pin and disk. The phenomenon was more obvious under an applied high load of 40 N testing condition.

Considering other excellent physical, chemical and mechanical properties of the Ni_3Al -based intermetallic materials, the present investigation has recognized that it will be meaningful and possible to develop Ni_3Al -matrix composites, reinforced by both hard Cr_3C_2 -particles and soft MnS-particles for tribological applications. Concerned to wear mechanism, composition development, influence of microstructure on tribological performance of the alloy system, further investigation is needed.

Acknowledgements

The authors are grateful for the financial support given by the Swedish VINNOVA and Chinese MOST for the international collaborative research projects P32737-1 and P32737-2, and appreciate the Department of Manufacturing Engineering and Engineering Management, City University of Hong Kong for allowance to use the facilities for tribological evaluation. Also, special tanks are directed to Mr. Lin Zhi, University of Science and Technology Beijing, for his fruitful assistance on high temperature hardness test.

References

- [1] A. Aoki, O. Izumi, J. Jpn. Inst. Met. 43 (1979) 1190.
- [2] R.N. Wright, J.R. Knibloe, Acta Metall. 38 (1990) 1993.
- [3] C.T. Liu, V.K. Sikka, J. Met. 38 (1986) 19.
- [4] C.T. Liu, C.L. White, Acta Metall. 35 (1987) 643.
- [5] J. Lapin, Intech 5 (1997) 615.
- [6] S. Ochiai, Y. Oya, T. Suzuki, Acta Metall. 32 (1984) 289.
- [7] R.W. Guard, J.H. Westbrook, Trans. AIME 215 (1959) 807.

- [8] C.T. Liu, Proceedings of the Symposium on High-Temperature Alloy Theory and Design, Bethesda, MD, April, 1984, pp. 9–11.
- [9] D.N. Tsipas, The effect of Hf additions on oxidation behaviour of Ni₃Al, in: The Third International Symposium on High-Temperature Corrosion of Metals and Alloys, Japan, November 18–20, 1982.
- [10] C.T. Liu, C.G. McKamey, ASM Materials Week '89, Indianapolis, Indiana, 2–5 October 1989.
- [11] B.J. Marquardt, J.J. Wert, Proc. Mater. Res. Soc. 39 (1985) 247.
- [12] P.J. Blau, C.E. DeVore, J. Tribol. 110 (1988) 646.
- [13] N.R. Bonda, D.A. Rigney, Proc. Mater. Res. 133 (1989) 585.
- [14] P.J. Blau, C.E. DeVore, Proceedings of the 1989 Wear of Materials Conference, American Society of Mechanical Engineers, 1989, p. 305.
- [15] P.J. Blau, C.E. DeVore, Tribol. Int. (1990) 226.
- [16] M. Johnson, D.E. Mikkola, P.A. March, R.N. Wright, Wear 140 (1990) 279.
- [17] Shangping Li, Di Feng, Heli Luo, Microstructure and abrasive wear performance of chromium carbide reinforced Ni₃Al matrix composite coating, Surf. Coat. Technol. 201 (2007) 4542–4546.
- [18] Compilatory group of machine-producing technology and material (Ed.), Handbook of Machine Producing Technology and Material (Second Part), Machine Industry Press, 1993, p. 674.
- [19] K. Gong, H. Luo, D. Feng, C. Li, Wear 265 (2008) 1751–1755.
- [20] J. Jiang, R.D. Arnell, Wear 218 (1998) 223–231.
- [21] Y. Liu, A. Erdemir, E.I. Meletis, Surf. Coat. Technol. 82 (1996) 48–56.
- [22] http://www.engineersedge.com/properties_of_metals.htm.
- [23] R.K. Williams, R.S. Graves, F.J. Weaver, D.L. McElroy, Metals and Ceramics' Division, O.R. National Lab. Oak Ridge, Tennessee.
- [24] D.A. Rigney, L.H. Chen, M.G.S. Naylor, A.R. Rosenfield, Wear 100 (1984) 195.
- [25] D.A. Rigney, M.G.S. Naylor, R. Divakar, L.K. Ives, Mater. Sci. Eng. 81 (1986) 409.
- [26] D.A. Rigney, in: R.A. Huggins (Ed.), Annual Review of Materials Science, Vol. 18, Annual Review Inc., Palo Alto, CA, 1988, p. 141.
- [27] B.H. Kear, H.G.F. Wilsdorf, Trans. Met. Soc. AIME 224 (1962) 382.
- [28] V. Paider, D.P. Pope, V. Vltek, Acta Metall. 32 (1984) 435.
- [29] S. Takeuchi, E. Kuramoto, Acta Metall. 21 (1973) 415.
- [30] D.P. Pope, S.S. Ezz, Int. Met. Rev. 29 (1984) 136.
- [31] Personal communication to Luo Heli, China Iron and Steel Research Institute Group Ltd.
- [32] Y.C. Chiou, K. Kato, Jpn. Soc. Lubr. Eng. Int. Ed. 9 (1988) 11–16.
- [33] T. Akagaki, D.A. Rigney, Wear 149 (1991) 353–374.